

Photometric Survey for Dwarf Galaxies Within Intergalactic Voids

Rochelle Steele

A senior thesis submitted to the faculty of
Brigham Young University
in partial fulfillment of the requirements for the degree of
Bachelor of Science

J. Ward Moody, Advisor

Department of Physics and Astronomy

Brigham Young University

April 2019

Copyright © 2019 Rochelle Steele

All Rights Reserved

ABSTRACT

Photometric Survey for Dwarf Galaxies Within Intergalactic Voids

Rochelle Steele

Department of Physics and Astronomy, BYU

Bachelor of Science

No astronomer has yet discovered the dwarf galaxies that many Λ Cold Dark Matter (Λ CDM) simulations predict should be abundant within intergalactic voids. Spectroscopic observations are necessary to identify and determine the distances to these galaxies. However, dwarf galaxies are so faint that it is difficult to observe them with spectroscopic methods. We have developed a way to photometrically identify dwarf galaxies and estimate their distance using three narrowband filters centered on the $H\alpha$ emission line. From this method, the redshift of the $H\alpha$ emission line can be estimated, which gives the distance to the galaxy. Equivalent width, or strength, of the emission line detected can also be estimated. The line observed must be verified as $H\alpha$ emission using observations with Sloan broadband filters. We have primarily studied one void, FN8, using these methods and have found 14 candidate dwarf galaxies, which must still be confirmed spectroscopically. The low density of candidate void galaxies rejects the hypothesis that there is a uniform distribution of dwarf galaxies within the void, as suggested by some Λ CDM simulations.

Keywords: large-scale structure, voids, dwarf galaxies, dark matter, Λ CDM

ACKNOWLEDGMENTS

I would first like to thank my advisor, Dr. J. Ward Moody, for his tireless help and support in this project. He has taught me a lot, not only through his tutelage, but through his kindness and example to me of what a good astronomer and person looks like.

I would also like to acknowledge the support of Chris Draper who has worked closely with me throughout this project and has taught me more than I could have learned on my own about large scale structure, dark matter and research skills.

Based on observations at Kitt Peak National Observatory, National Optical Astronomy Observatory (2014A-0343, 2014B-0178; PI: J. Moody), which is operated by the Association of Universities for Research in Astronomy (AURA) under cooperative agreement with the National Science Foundation. The authors are honored to be permitted to conduct astronomical research on Iolkam Du'ag (Kitt Peak), a mountain with particular significance to the Tohono O'odham.

I thank Stephen McNeil, Michael D. Joner and Jackson Steele, who made necessary and significant contributions to this research.

I gratefully acknowledge the financial support of the College of Physical and Mathematical Sciences for my work in this project.

Finally, I would like to thank the Department of Physics and Astronomy for the education I have received in physics and astronomy, without which I would not have been able to conduct this research.

Contents

Table of Contents	iv
List of Figures	vi
1 Introduction	1
1.1 Λ CDM Model of the Universe	1
1.1.1 Dark Matter: Hot and Cold (and Warm)	2
1.1.2 Physical Predictions	2
1.1.3 The Dwarf Galaxy Problem	3
1.2 Distance Measurements	4
1.3 Previous Work	9
2 Methods	11
2.1 Narrowband filters	11
2.2 Finding and Narrowing Candidates	13
2.2.1 Source Extractor	13
2.2.2 Visual Survey	14
2.2.3 Systematic Classification	16
2.3 Calibrating EW and cz from ratios	17
2.4 Broadband Filters	21
3 Results and Discussion	24
3.1 Results	24
3.2 Analysis	25
3.3 Conclusions	27
3.4 Future Work	27
Appendix A Systematic Classification Code - VBA	29
A.1 CountKeep_Click()	29
A.2 EW_Click()	30
A.3 FillInFormulas_Click()	30
A.4 FindConstant_Click()	38

A.5	FindCorrelation_Click()	40
A.6	MagErrKeep_Click()	41
A.7	MinValue_Click()	42
A.8	PhysicalCheck_Click()	42
A.9	SelectColumn_Click()	43
A.10	StDevAndMedian_Click()	44
Appendix B Expected Numbers Code - MATLAB		46
B.1	ExpectedNumberofGalaxiesTOTAL.m	46
B.2	ExpectedNumberofGalaxiesHa.m	49
B.3	ExpectedNumberofGalaxiesOIII.m	53
B.4	ExpectedNumberofGalaxiesOII.m	56
B.5	Schechter.m	60
Bibliography		61
Index		63

List of Figures

1.1	HDM, WDM and CDM	3
1.2	Galaxy Spectrum	5
1.3	Redshift Analogy	6
1.4	Galaxy Photometry	8
2.1	Narrowband Transmission	12
2.2	H α Frames example	15
2.3	Ratios to EW and cz	18
2.4	Natural Neighbor Example	19
2.5	Broadband Relationship	22
3.1	Expected Numbers Distance	26

Chapter 1

Introduction

1.1 Λ CDM Model of the Universe

The Λ Cold Dark Matter (Λ CDM) model of the universe, a widely accepted model, describes what the universe is made of and how galaxies should be arranged within it. It is based on the idea that the universe is made up of three different types of energy or mass (with energy and mass being thought of interchangeably): baryonic matter, cold dark matter and dark energy (Λ). Baryonic matter is the “regular” matter that can be seen (eg., stars, galaxies, interstellar gas). Dark matter is a type of matter that cannot be directly observed because it does not interact with electromagnetic (EM) waves (i.e., light). The only way dark matter interacts with baryonic or normal matter is gravitationally. Dark energy is the unknown energy that is causing the acceleration of the expansion of the universe. According to the Planck mission, dark energy makes up 71.9% of the universe’s energy and dark matter is 23.5%, leaving regular matter as only 4.6% of what makes up the universe (Hinshaw et al. 2013).

1.1.1 Dark Matter: Hot and Cold (and Warm)

Dark matter is an essential component of galaxy formation. Because dark matter can still interact with baryonic matter gravitationally, clumps of dark matter attract baryonic matter which eventually collapses to create stars and galaxies. The nature of dark matter influences how these galaxies are formed. One important aspect of dark matter is its temperature.

Temperature of dark matter describes the energy and speed of the unknown particles. Dark matter particles that move at relativistic speeds are termed hot dark matter (HDM) (Carroll & Ostlie 2007). Particles that move slow enough that astronomers can neglect their random motions are termed cold dark matter (CDM) (Maran 1992). If a dark matter particle has speed between that of cold and hot dark matter, it is termed warm dark matter (WDM). Determining the actual temperature of dark matter can be done by observing how dark matter interacts with baryonic matter.

Each type of dark matter affects galaxy formation differently. HDM moves so fast that it spreads out, making it harder for small galaxies to form. In an HDM universe, galaxies form "top-down" meaning that structures form in large gas clouds first, then break up to make normal galaxies. In a CDM universe, dark matter clumps more easily, which attracts more baryonic matter to it. This makes it possible for small dwarf galaxies to form, making a "bottom-up" formation method, where small galaxies form first, then combine to make normal galaxies. Dwarf galaxies are abundant in a CDM universe. WDM works similarly to CDM, but creates fewer small galaxies.

1.1.2 Physical Predictions

Large-scale structure (LSS) is how galaxies are arranged throughout the universe. Figure 1.1 highlights the physical differences that cold, warm or hot dark matter would have on the LSS. The images in Figure 1.1 are of different simulations of the dark matter in the universe and show the density of the universe, with pink and purple representing high density areas and blue representing low density areas. The simulation for the left panel uses HDM, the middle panel uses WDM and

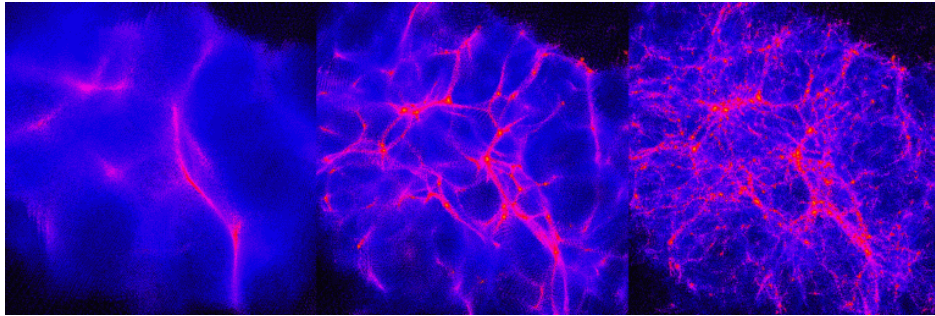


Figure 1.1 Simulations of how the density of the universe would appear with different types of dark matter. The pink/purple colors represent areas of high density while the blue colors are areas of low density. The left panel uses HDM, the middle panel uses WDM and the right panel uses CDM. Simulations by Ben Moore (University of Zurich).

the right panel uses CDM.

Simulations using the Λ CDM model, which assumes CDM (shown on the right panel of Figure 1.1), have been able to accurately reproduce many properties of the observed universe, including star formation rate (the rate at which stars are being formed), the brightness of galaxy clusters or groups and how galaxies evolve over time (J. S. Bullock 2017; Schaye et al. 2015; Vogelsberger et al. 2014). From these and other successes of the Λ CDM simulations, the Λ CDM model is preferred over WDM and HDM. There are, however, still issues with the model.

1.1.3 The Dwarf Galaxy Problem

Dwarf galaxies are galaxies that are many times smaller than our own Milky Way and are mostly gas and dust, with very few stars. These types of galaxies form very easily with CDM, but would be almost impossible to create with HDM. Consequently, the Λ CDM model predicts there should be many dwarf galaxies, while WDM predicts fewer dwarf galaxies and HDM predicts almost none at all. One place that Λ CDM predicts there should be an abundance of dwarf galaxies is within cosmic voids.

The large-scale structure of the universe is full of clusters and filaments rich with galaxies, as

can be seen in purple in Figure 1.1. Between these densely populated areas, there are, naturally, low density regions, called voids (which are the blue regions of Figure 1.1), with no sizable galaxies in them. The Λ CDM model predicts, however, that there should be an abundance of dwarf galaxies within these intergalactic voids. Observations thus far have not found any. This may be because of a real discrepancy between the simulations and observations or simply a bias in the observation methods, since these galaxies are incredibly faint. The goal of this research is to survey for these faint dwarf galaxies to determine if the voids are, in fact, void.

1.2 Distance Measurements

When determining if an observed galaxy is in a void, it is important to know how far away the galaxy is, otherwise you may be observing an object in front of or behind the void. But, measuring distance in astronomy is difficult, to say the least. No ruler spans from Earth to the Moon, let alone from us to a distant dwarf galaxy in the early universe. All that astronomers have to work with is the light that is received from an object, and a nearby dim galaxy looks a lot like a distant bright one.

One tried and true method to determine distance in cosmology is spectroscopy. Spectroscopy is a method of observation where the light received by the telescope is split into its component wavelengths to produce a spectrum. Each galaxy spectrum contains certain emission and absorption lines. An example of the spectrum of a galaxy with emission is shown in Figure 1.2. These emission lines correspond to specific atomic transitions with known wavelengths. For example, the $H\alpha$ emission line, displayed in Figure 1.2, has a wavelength of 6563 Å and comes from the first transition in the hydrogen Balmer series. Other emission lines present in the spectrum in Figure 1.2 include the $[OIII]\lambda 5007,4959$ doublet (double line) from doubly ionized oxygen and the $[OII]\lambda 3726,3729$ doublet from singly ionized oxygen. The numbers after the “ λ ” refer to the wavelengths of those lines in Ångstroms. For the purposes of this paper, I will treat the $[OIII]\lambda 5007,4959$ doublet as a

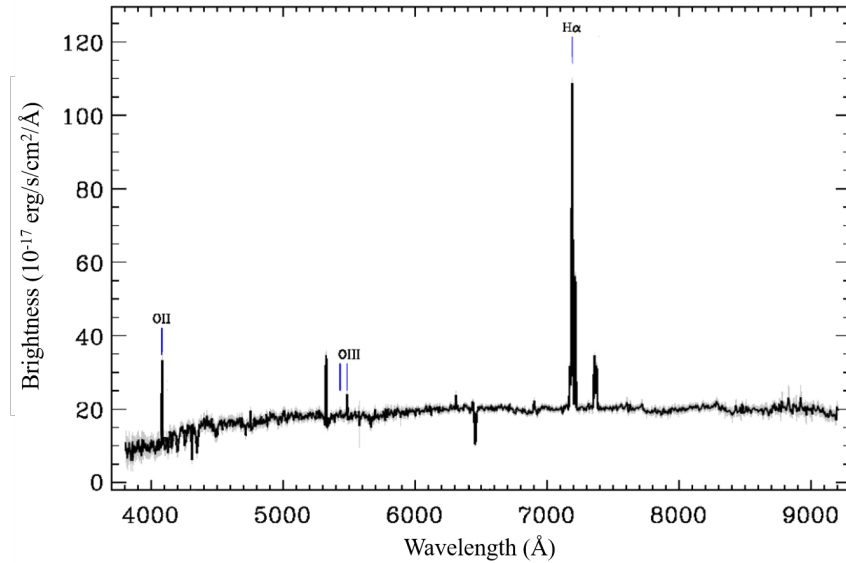


Figure 1.2 The spectrum of a sample galaxy from Sloan Digital Sky Survey (SDSS). The x-axis gives the wavelength of light. The y-axis gives the brightness measured at that wavelength in $\text{erg/s/cm}^2/\text{\AA}$. These units represent a power (erg/s) per unit area (cm^2) at a given wavelength (\AA). This galaxy has a number of emission lines present, including the first in the Balmer series of hydrogen, called the $\text{H}\alpha$ line; the $[\text{OIII}]$ line, from doubly ionized oxygen; and the $[\text{OII}]$ line, from singly ionized oxygen. The emission lines have been shifted to longer wavelengths because of cosmological redshift, which is explained below. This figure is adapted from Abolfathi et al. (2018).

single $[\text{OIII}]$ line and the $[\text{OII}]\lambda 3726,3729$ doublet as a single $[\text{OII}]$ line. Both of these oxygen lines are indicated on Figure 1.2. All galaxies with regions of ionized hydrogen, such as dwarf galaxies, have similar spectra, so the emission lines present in a galaxy's spectrum can be easily identified.

One important aspect of spectra is the width or strength of the emission lines. This is calculated with the quantity equivalent width (EW). To find the EW, the spectrum must be normalized so that the continuum curve under the emission lines is set equal to one. A rectangle with the same height as the continuum and the same area as the emission line is modeled. The width of that rectangle is the EW. We expect the dwarf galaxies in the void to have emission lines, but the emission may be of varying strength, which is why EW must be taken into account when dealing with spectral lines.

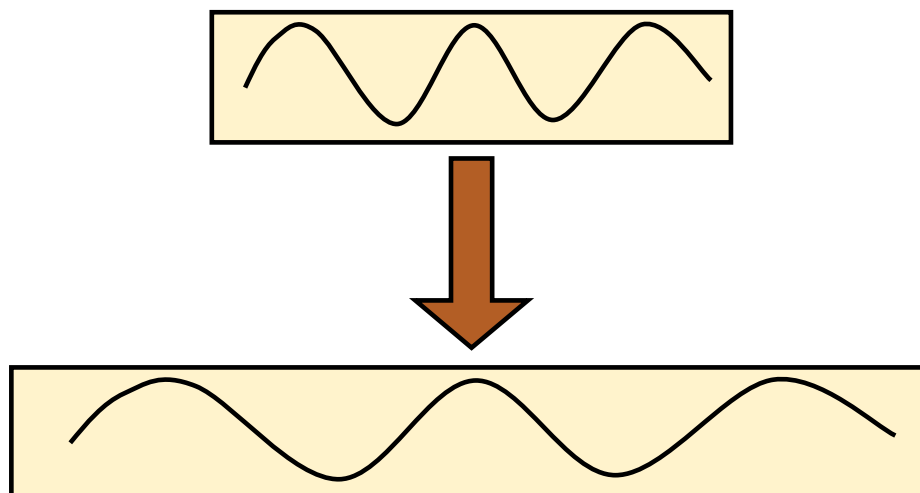


Figure 1.3 This figure shows one rubber band with a wave drawn on it before (top) and after (bottom) the rubber band has been stretched. The stretching of the rubber band (analogous to the expansion of spacetime) in turn makes the wave appear to have a longer wavelength (analogous to the cosmological redshifting of light).

These spectral lines are not always where they are expected to be because of cosmological redshift. This line shifting can be observed in Figure 1.2. The universe is not static, but expanding. It's not simply that the objects inside space, such as stars and galaxies, are moving away from each other; spacetime itself is stretching. As light travels from distant galaxies, the space it travels through gets stretched. This expansion also stretches the light, giving the light a longer wavelength than it started with. The longer wavelength makes the light we receive from other galaxies appear more red than it actually is.

One helpful way to visualize cosmological redshift is by imagining a wave drawn on a rubber band (Figure 1.3). The rubber band represents spacetime and the wave represents a wave of light. The upper rubber band shows the wave before any redshifting. As the universe expands, the rubber band gets stretched. Notice that the drawing of the wave itself is not being stretched, the rubber band is. But because the drawing is on the rubber band, the wave gets stretched right along with it. This is the same for cosmological redshift. The light is only stretched because it is coupled with spacetime and spacetime has been stretched. The resulting wave, shown on the bottom of Figure

1.3, has a longer wavelength than the original wave and therefore appears more red.

The amount by which the light has been stretched or "redshifted" is proportional to how far away it originated. For relatively nearby objects, the relationship between redshift and distance is

$$cz = H_0 d, \quad (1.1)$$

where z is the redshift, H_0 is the Hubble constant (for our purposes, $H_0 = 70 \text{ km s}^{-1} \text{Mpc}^{-1}$), c is the speed of light in km/s and d is the distance to the galaxy in Mpc (1 Mpc = 1 Megaparsec = 3.26×10^6 lightyears). The quantity cz is loosely referred to as redshift, but is actually an estimate of the speed of the galaxy being observed as it is pulled away from us by the expansion of spacetime. This estimate of the galaxy's speed is only accurate for very low redshift ($z \ll 1$).

Astronomers use the relationship in Equation 1.1 to determine the distances to galaxies once redshift is known. Redshift can be determined spectroscopically. With spectroscopic observations, scientists calculate how much the emission lines have been shifted from their emitted or rest wavelength. The redshift is found from the relationship

$$z = \frac{\Delta\lambda}{\lambda_{\text{em}}} = \frac{\lambda_{\text{obs}} - \lambda_{\text{em}}}{\lambda_{\text{em}}}, \quad (1.2)$$

where λ_{obs} is the observed wavelength and λ_{em} is the rest wavelength. The calculated redshift is then used to determine the distance to the galaxy being observed, using Equation 1.1.

While accurate, spectroscopy has its drawbacks. First, a lot of light is required, so spectroscopy needs long exposures, especially to observe dim objects. Second, spectroscopy is an inefficient way to survey a large area of the sky because it is usually done one object at a time.

Photometry, a different method of astronomical observations, offers different advantages. Photometry is the imaging of a field of stars or galaxies using filters. These filters only let in a certain bandpass of wavelengths (e.g., only red light or only UV light). An example of a photometric image is shown in Figure 1.4. Figure 1.4 is a composite or sum of many photometric images taken in different filters. The galaxy pointed out by the red arrow is the same galaxy whose spectrum is

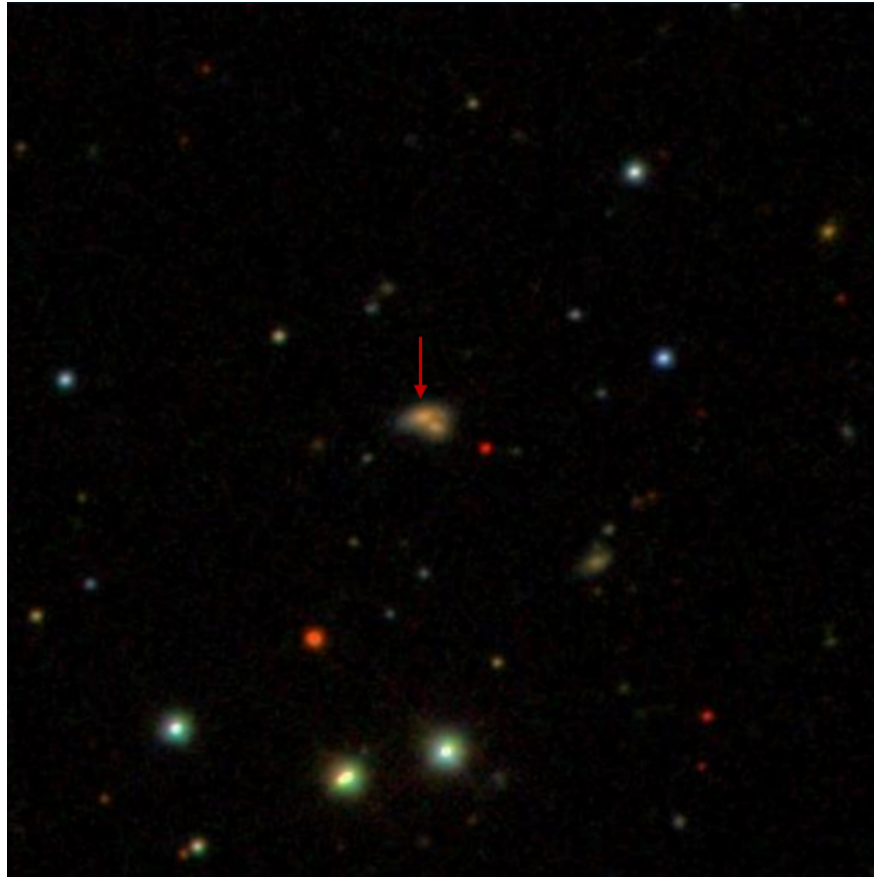


Figure 1.4 A composite of many photometric images of the same sample galaxy in Figure 1.2 from Sloan Digital Sky Survey (SDSS). The galaxy is in the center of the frame. Abolfathi et al. (2018)

shown in Figure 1.2. Photometric observations can be done more quickly but do not give scientists as much information. Instead of giving a spectrum of one object, it gives a one color image of multiple objects.

We have developed a method to accurately determine distance with photometry. This method is ideal for void galaxy surveys because photometry can more easily detect faint objects, such as dwarf galaxies. We have applied this method to find dwarf galaxies within voids.

1.3 Previous Work

Many studies have been done to investigate the dwarf galaxy problem discussed in Section 1.1.3. According to a number of simulations, like the one done by Tikhonov & Klypin (2009), the Λ CDM model predicts an overabundance of dwarf galaxies within cosmic voids. Tikhonov & Klypin (2009) found that a factor of ten more halos were predicted by their Λ CDM simulation than are found by observations.

However, not all simulations have predicted this same disparity. Tinker & Conroy (2009) found that the gap between current observations and Λ CDM simulations could be closed by accounting for galaxy bias. The structure of baryonic matter in the universe does not exactly follow the layout of dark matter. This difference is called a galaxy bias. A galaxy bias requires that the mass of a group of dark matter, called a dark matter halo, reach a certain lower limit before it is massive enough to attract baryonic matter to form a galaxy or dwarf galaxy. The work done by Tinker & Conroy (2009) implies that there is dark matter within the voids, as predicted by the Λ CDM model, just not enough to form dwarf galaxies there.

Another theory suggests that there are other factors from areas around the voids that are quenching star and galaxy formation within the void. Simpson et al. (2013) studied the effects of supernova feedback and UV background radiation on star formation within dwarf galaxies. Supernovae, or exploding stars, in the filaments and clusters surrounding the voids push whatever gas may be within the voids out of them. UV radiation, from a variety of sources in the early universe, heat and ionize the gas in early dwarf galaxies, pushing that gas out of the galaxy and void as well. Simpson et al. (2013) showed that supernovae feedback and reionization from UV background radiation are able to quench star formation in dwarf galaxies.

In 2014, Draper et al. (2019), from BYU, took narrowband and broadband image data of nearby voids to see if this data can be used to identify dwarf galaxies and estimate their distances. A description of the narrowband filters used in these observations can be found in Section 2.1. Section

2.2 lays out the methods we used to narrow potential void galaxy candidates. The calibrations of our method are discussed in Sections 2.3 and our verification method, using broadband filters is described in Section 2.4. Chapter 3 presents the results, with Section 3.1 covering our results, Section 3.2 analyzing these results and Section 3.3 drawing conclusions from the work. Section 3.4 discusses how this work could be furthered.

Chapter 2

Methods

2.1 Narrowband filters

The Kitt Peak National Observatory (KPNO) owns a precise set of redshifted $H\alpha$ filters for survey work. We used three of these narrow 80\AA wide Gaussian filters called $H\alpha 8$, $H\alpha 12$ and $H\alpha 16$. The $H\alpha 8$, $H\alpha 12$ and $H\alpha 16$ filters have been shifted 8 nm, 12 nm and 16 nm from the rest wavelength of the $H\alpha$ line, respectively. A plot of the transmissions of these filters is shown in Figure 2.1. The vertical dashed lines in the figure refer to where the $H\alpha$ emission line of a galaxy would appear if that galaxy were at the given redshift. The left most dashed line ($cz=3200$ km/s) marks the front of the void observed and the right most dashed line ($cz=6800$ km/s) marks the back edge of the void.

Observations were taken through the $H\alpha$ filters using the KPNO Mayall 4-m telescope and Mosiac 1.1 Wide Field Imager. We observed the voids FN8 and FN2 (primarily FN8) from the Foster-Nelson catalog (Foster & Nelson 2009) because the $H\alpha$ line of a hypothetical galaxy within those voids would be redshifted by about 12 nm, directly in the bandpasses of our filters, as illustrated in Figure 2.1. Images of objects provided photon counts in each filter, meaning the amount of light collected. We used the ratios of the counts from different filters for each object to

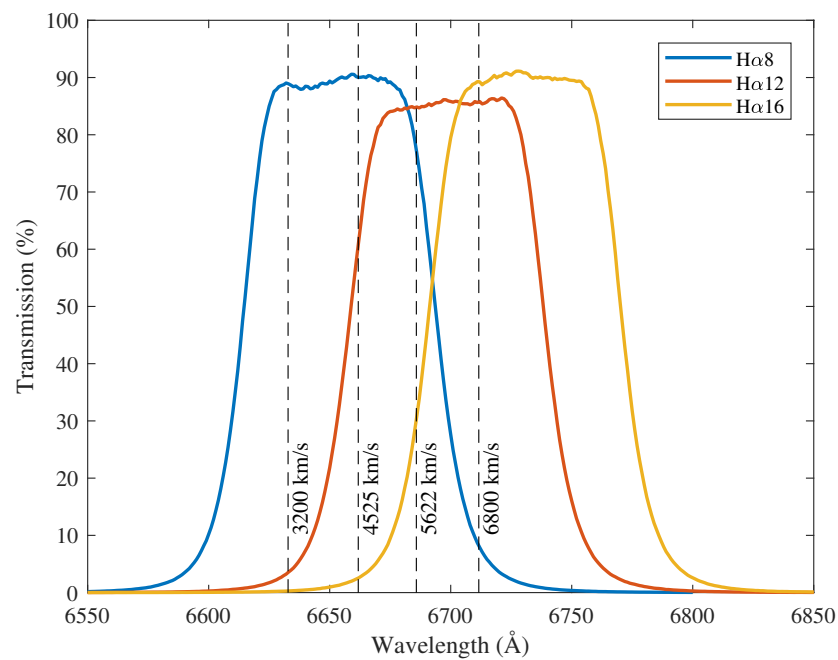


Figure 2.1 A plot of the transmission (percentage of light allowed through) for each filter ($H\alpha 8$, $H\alpha 12$, $H\alpha 16$) with respect to wavelength. The transmissions of $H\alpha 8$, $H\alpha 12$ and $H\alpha 16$ are marked in blue, red and yellow, respectively. The dotted black lines represent where the $H\alpha$ line would be at the marked redshifts. The front edge of the void FN8 is at $cz = 3200$ km/s and the back edge of the void is at $cz = 6800$ km/s.

estimate their redshift. The ratios used were $H\alpha_{12}/H\alpha_8$ and $H\alpha_{12}/H\alpha_{16}$.

To illustrate the function of these ratios, imagine a galaxy at the redshift $cz = 4000\text{km/s}$. This puts the $H\alpha$ emission line in the middle of the bandpass of the $H\alpha_8$ filter (see Figure 2.1). The counts detected by the $H\alpha_8$ filter are then much higher than the counts detected by the $H\alpha_{12}$ or $H\alpha_{16}$ filters, because of the presence of the emission line. This means that $H\alpha_{12}/H\alpha_8 < 1$, while $H\alpha_{12}/H\alpha_{16} \approx 1$, indicating the dwarf galaxy is in the front third of the void. Similarly, dwarf galaxies at different redshifts result in the $H\alpha$ lines being shifted by different amounts, causing the $H\alpha_{12}/H\alpha_8$ and $H\alpha_{12}/H\alpha_{16}$ ratios to vary. Section 2.3 goes into the specifics of how the redshift and equivalent width of the line are uniquely determined from the $H\alpha_{12}/H\alpha_8$ and $H\alpha_{12}/H\alpha_{16}$ ratios.

2.2 Finding and Narrowing Candidates

There were 12 fields of view in both FN8 and FN2 imaged, with each field covering 0.25 deg^2 of the sky. Within each field, tens of thousands of objects had to be identified and classified to determine if they were void galaxy candidates. Potential galaxies were originally identified with a program called Source Extractor, described in Section 2.2.1. Void galaxy candidates were also identified visually, which is described in Section 2.2.2. Finally, the objects found by Source Extractor were systematically classified to narrow down potential candidates, as described in Section 2.2.3.

2.2.1 Source Extractor

Source Extractor (Bertin & Arnouts 1996) is a program used to identify galaxies from photometric images. The program scans the image and, extracts the counts of all the objects above a given count threshold.

The summed image from the $H\alpha_8$, $H\alpha_{12}$ and $H\alpha_{16}$ filters was fed into Source Extractor which

generated a list of coordinates for each object and their brightness, or counts, in each filter. We then formed a list of void candidates from the Source Extractor data and calculated the ratios of these counts ($H\alpha_{12}/H\alpha_8$ and $H\alpha_{12}/H\alpha_{16}$). Each candidate had to be confirmed visually.

2.2.2 Visual Survey

The visual survey was one of my responsibilities. Each field was imaged in three filters, as described in Section 2.1. Figure 2.2 gives a small portion of a field of view in the original three filters, $H\alpha_8$ on the bottom left, $H\alpha_{12}$ on the bottom center and $H\alpha_{16}$ on the bottom right. To determine which of the many objects in view could be within the void, I subtracted the images from each other to get an $H\alpha_{12}-H\alpha_8$ image and an $H\alpha_{12}-H\alpha_{16}$ image (the top center and top right images in Figure 2.2, respectively). I used subtracted images for the visual survey instead of the ratios ($H\alpha_{12}/H\alpha_8$ and $H\alpha_{12}/H\alpha_{16}$) used for the rest of the method because the difference between the filters is related to the ratios and is easier to use when visually identifying objects. The upper left image in Figure 2.2 is the composite image, used by Source Extractor, of the three original images in the filters. The composite frame was used to verify that the objects identified were real objects and not simply an artifact of the subtraction process.

With the subtracted images, I manually scanned each field searching for an object that looked like a void galaxy. If the object was within the void, the $H\alpha_{12}$ filter was brighter than the $H\alpha_8$ filter, $H\alpha_{16}$ filter or both, meaning that, in the subtracted images, the desired galaxies appeared as white spots. This is the case when the emission line is in the bandpass of the $H\alpha_{12}$ filter in Figure 2.1, but not the $H\alpha_8$ or $H\alpha_{16}$ filters. An example of one of these objects is shown in the red circles in Figure 2.2. Regular stars and galaxies that did not have an emission line where we expected (and were therefore not within the void) appeared as black spots or were subtracted out completely because the counts in all the filters would be about the same.

This method was created for dim objects (i.e., dwarf galaxies), so brighter objects are saturated

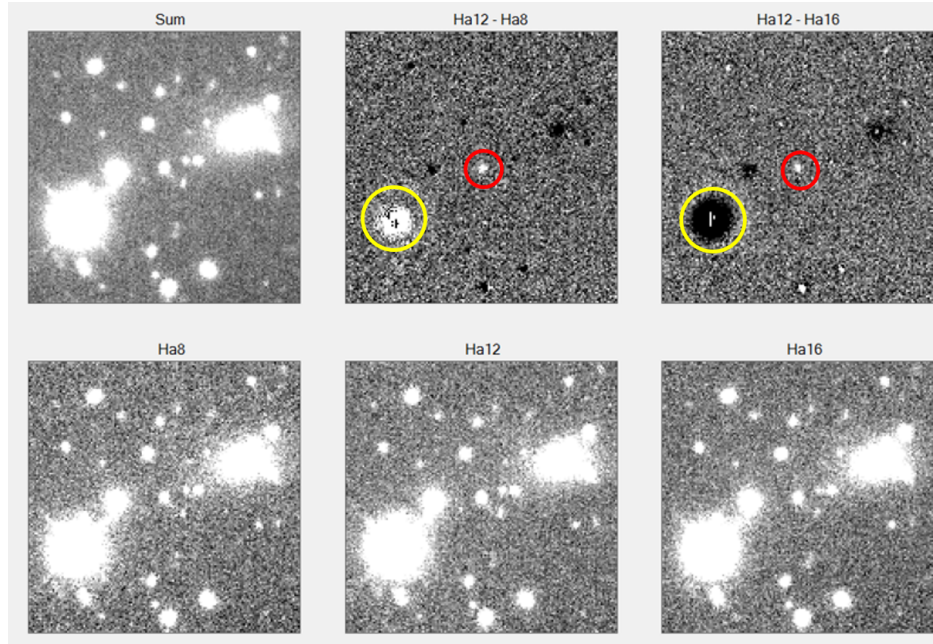


Figure 2.2 An example of the six frames necessary for visual observations. The images on the bottom panel are the original images from the $H\alpha 8$, $H\alpha 12$ and $H\alpha 16$ filters (left to right). The top left frame is a composite of all three images. The top center frame is the difference between the $H\alpha 12$ and $H\alpha 8$ filters and the top right frame is the difference between the $H\alpha 12$ and $H\alpha 16$ filters. The object within the red circles is a void galaxy candidate. The object in the yellow circles is not a void galaxy candidate and has saturated the pixels (i.e., it is too bright).

in the image. Saturation means that the pixels have received more light than can be accurately recorded, so the data for that object are not reliable. An example of a saturated object is the object within the yellow circles in Figure 2.2. Because this star is saturated, the subtraction image $H\alpha 12 - H\alpha 8$ shows a white spot. The dark spot in the center of the object in the $H\alpha 12 - H\alpha 8$ image is the telltale sign that, although the object appears white like the void galaxies, it is not a void galaxy and should be discarded.

For each field of view, I found up to a few dozen objects. Those found in the visual survey were marked so that they were not accidentally discarded by the systematic classification.

2.2.3 Systematic Classification

The visual survey was a qualitative way to verify that our systematic classification was accurate. The systematic classification used more quantitative measurements. The list of candidates found with Source Extractor (see Section 2.2.1 for more detail on Source Extractor) served as a starting point for this method. But, of the tens of thousands of objects found by Source Extractor, only a few were valid void galaxy candidates. Quantitative criteria were used to narrow down this list so that only the objects most likely to be within the void remained. These criteria included a minimum count value and a requirement that the $H\alpha_{12}/H\alpha_8$ and $H\alpha_{12}/H\alpha_{16}$ were close to the desired values.

The systematic method was originally very hands-on, requiring that I manually verify the parameters for the candidate dwarf galaxies and delete the objects that didn't meet the criteria. This process took up to an hour for one field of view, and left room for human error. Because of this, I decided to automate the process by writing a code in Visual Basic for Applications (VBA) to take over what I had been doing by hand.

The VBA code I created performed all the commands needed to test the parameters of the objects found by Source Extractor. This code is printed in Appendix A. Many parameters were calculated from the given Source Extractor data. The candidate galaxies were then sorted by these parameters and classified as a void galaxy candidate or deleted as a false positive. Below are a list and explanations of many of the parameters used.

Magnitude Error Check. The error in the magnitude, or brightness, measurement given by Source Extractor was found. If it was above a certain value, the object was deleted.

Minimum Count Check. The counts, or amount of light received by the telescope, in each filter were checked against a minimum value. If the counts from all of the filters were below the minimum value, the object was deleted.

Physical Object Check. Some of the objects identified by Source Extractor could simply be defects on the image. To find and reject some of these, the VBA code inspected the $H\alpha_{12}/H\alpha_8$ and

$H\alpha_{12}/H\alpha_{16}$ ratios. If both $H\alpha_{12}/H\alpha_8 < 1$ and $H\alpha_{12}/H\alpha_{16} < 1$, that would mean the spectrum of that object dips in the $H\alpha_{12}$ filter. This signature is not physical so the object can be disregarded.

Multivariate Cut. The candidates left are plotted on a graph with the $H\alpha_{12}/H\alpha_8$ ratio on the x-axis and the $H\alpha_{12}/H\alpha_{16}$ ratio on the y-axis. Objects with both of their $H\alpha$ ratios close to one are most likely stars or bright galaxies, neither of which are the dwarf galaxies for which we are searching. Once plotted on the graph, the code deleted the 95% of objects closest to the point $H\alpha_{12}/H\alpha_8 = 1$ and $H\alpha_{12}/H\alpha_{16} = 1$, leaving only the 5% with the desired hydrogen ratios.

Once the VBA code was written and working properly, the time spent on each field was brought down to about five minutes or less and made the entire process much easier to accurately duplicate for future work with this method. Through these systematic classifications, the original list of tens of thousands of objects per field was reduced to a couple hundred candidates.

2.3 Calibrating EW and cz from ratios

The ratios $H\alpha_{12}/H\alpha_8$ and $H\alpha_{12}/H\alpha_{16}$ map to a unique equivalent width (EW), or line strength, and redshift (cz) for a given emission line from a galaxy. Figure 2.3 gives a general view of this mapping. The x-axis is the $H\alpha_{12}/H\alpha_8$ ratio and the y-axis is the $H\alpha_{12}/H\alpha_{16}$ ratio. The curved, colored lines show how the EW maps with the hydrogen ratios. The dark, dashed lines mark the redshift and show its relationship to the hydrogen ratios. This relationship between redshift and EW and the hydrogen ratios must be specific or else a valid estimate of the redshift (or distance) and EW (an indicator of emission line strength) could not be made. The specific relationship between these two values had to be modeled.

There were two steps to the modeling: model the ratios for a series of galaxy spectra of varying cz and EW and interpolate between those values to get a greater resolution.

To calibrate the relationship between the $H\alpha$ ratios and the redshift and EW of our models,

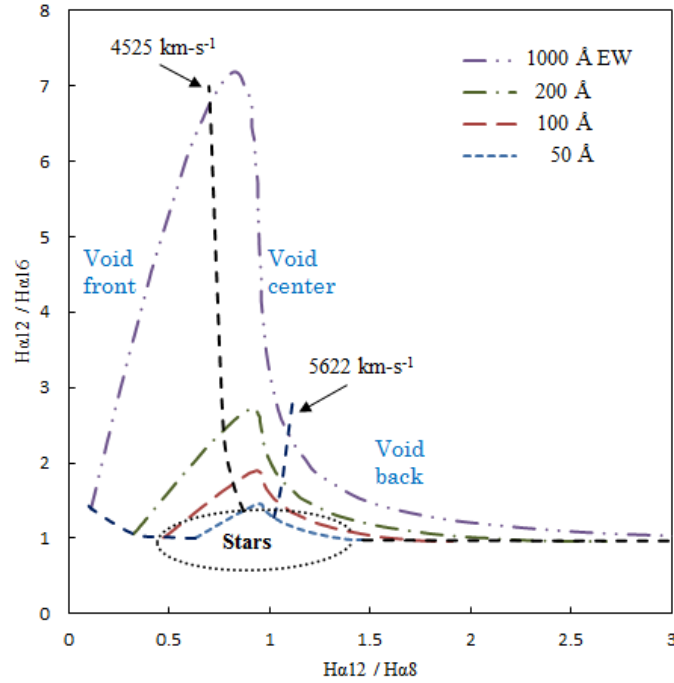


Figure 2.3 The mapping of the $H\alpha_{12}/H\alpha_{8}$ and $H\alpha_{12}/H\alpha_{16}$ ratios to equivalent width (EW) and redshift (cz). The x-axis represents the $H\alpha_{12}/H\alpha_{8}$ ratio and the y-axis represents the $H\alpha_{12}/H\alpha_{16}$ ratio. The colored curved lines are difference values for EW and the black dotted lines are difference values of redshift. Figure from Draper et al. (2019).

a galaxy spectrum with a known EW was modeled at a given distance and redshift. The $H\alpha$ ratios were then calculated for what we would expect to see from an object in that situation, thus identifying the relationship between the $H\alpha$ ratio values and the EW and redshift. This was done for many different redshift and EW values.

These values were used to begin to populate or “seed” two grids. Each grid had $H\alpha_{12}/H\alpha_{8}$ on one axis and $H\alpha_{12}/H\alpha_{16}$ on the other axis, similar to Figure 2.3. One grid mapped EW values and the other mapped redshift values. Once the grids were adequately seeded, we interpolated between the known values. The method used was a polynomial method where a polynomial was fit to each column of the grid, another was fit to each row of the grid and the two values were averaged together at each point on the grid.

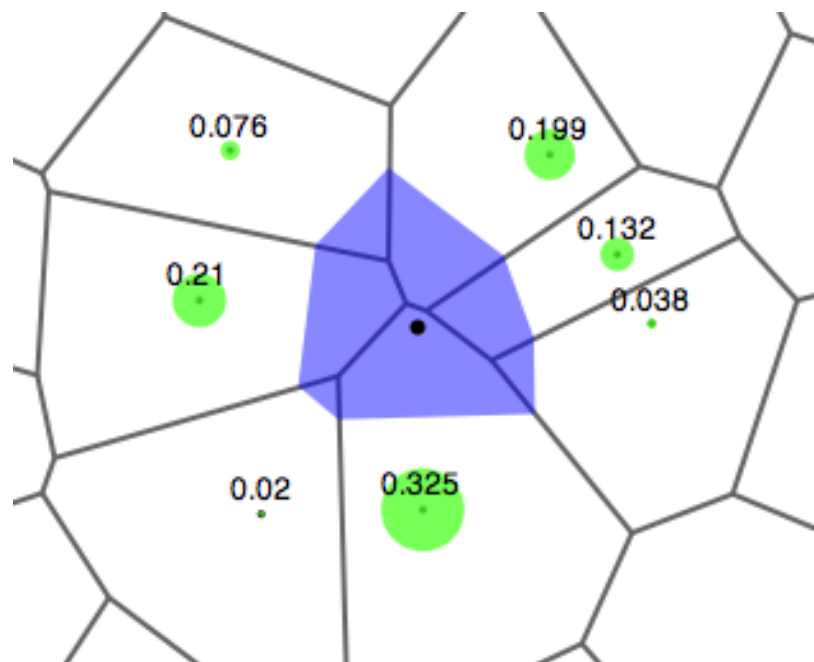


Figure 2.4 An example of Voronoi tessellations as used for the natural neighbor interpolation method. The white cells are the Voronoi cells of the original data points (marked within the center of each cell). The purple cell is the Voronoi cell for the query point (which is that black dot in center of frame). The numbers by each data point are the weights used in the weighted sum to estimate the value of the query point. These weights are the fraction of the purple cell that is overlapping the Voronoi cell of the corresponding data point. Figure by Markluffel, distributed by CC BY-SA 3.0 license.

Table 2.1 Six dwarf galaxies are described. Column 1 identifies each object. Column 2 shows our calculated equivalent width (EW) while Column 3 has the EW as determined spectroscopically by the Gemini telescope. Column 4 gives the redshift (cz) determined from our method and Column 5 has the redshift from the Gemini telescope.

ID	Our EW (Å)	Gemini EW (Å)	Our cz (km/s)	Gemini cz (km/s)
9573	240	251	6085	6122.306
19127	54	77	5915	5801.76
4837	71	83	6200	6353.442
6095	151	90	6060	6495.113
12858	60	58	6200	6099.736
20192	151	115	6060	6377.28

I tried many other methods that I thought would be more accurate than the polynomial method. These methods all used the natural neighbor interpolation method. Natural neighbor interpolation estimates the value of each query point by taking a weighted sum of the nearest seed data. The weights are determined with Voronoi tessellations. An example of the process is shown in Figure 2.4. Voronoi tessellations break up a grid interspersed with data into cells based on how close each grid point is to the seed data. The Voronoi cell of a data point is all the region around it which is closer to that data point than any other. For the natural neighbor method, Voronoi cells are created for the original data set; these are the white cells in Figure 2.4. A query point (the black dot in the center of Figure 2.4) is then placed into the grid. A Voronoi cell is created for this query point (the purple cell in Figure 2.4) and overlaid on the original Voronoi tessellation. The weight of each data point is the fraction that the new Voronoi cell overlaps with the Voronoi cell of that data point. The nearest neighbor method produces smooth interpolations that should match the original data well. Surprisingly, the polynomial method matched the true values better than any of the natural neighbor models.

Using the narrow Gaussian filters described in Section 2.1 and the polynomial interpolation method, we determined values for EW and redshift for the most promising objects. Six of these objects have been observed spectroscopically with the Gemini telescope to determine the true EW and redshift. Table 2.1 compares our values for EW and redshift to the measurements from Gemini. Note that the redshift from Gemini is determined with the assumption that the emission line being observed is $H\alpha$. While this was not the case for any of the six objects, doing this allowed us to determine that the accuracy of our method was 121 km/s. This is better accuracy than can usually be achieved in cosmology and better than the value we were expecting of about 300 km/s.

2.4 Broadband Filters

Even after calculating an estimated redshift and EW, there is still a chance that the candidates could be false positives. This is because there are objects far behind the void which, if at the correct distance, could have a different emission line redshifted to the wavelength where $H\alpha$ is expected. Specifically, there are two lines that could cause this: [OIII] and [OII]. Both of these lines can be seen in Figure 1.2. The [OIII] doublet is from doubly ionized oxygen and the [OII] doublet is from singly ionized oxygen.

To sift through these false positives, observations of the galaxies in broadband filters are used. The filters used are Sloan g' , r' and i' filters, where the g' is the green filter, r' is the red filter and i' is the infrared filter. From these images we compare the color indices. Color indices determine the color of an object by taking the difference in magnitude, or brightness, of that object in different filters. The color indices used were $g'-r'$ and $r'-i'$. Based on these color indices, we can predict if the galaxy in question is an $H\alpha$, [OIII] or [OII] emitter.

To calibrate the broadband method, Figure 2.5 was assembled using test galaxies chosen from the Sloan Digital Sky Survey (SDSS), a database that has photometric and spectroscopic data for

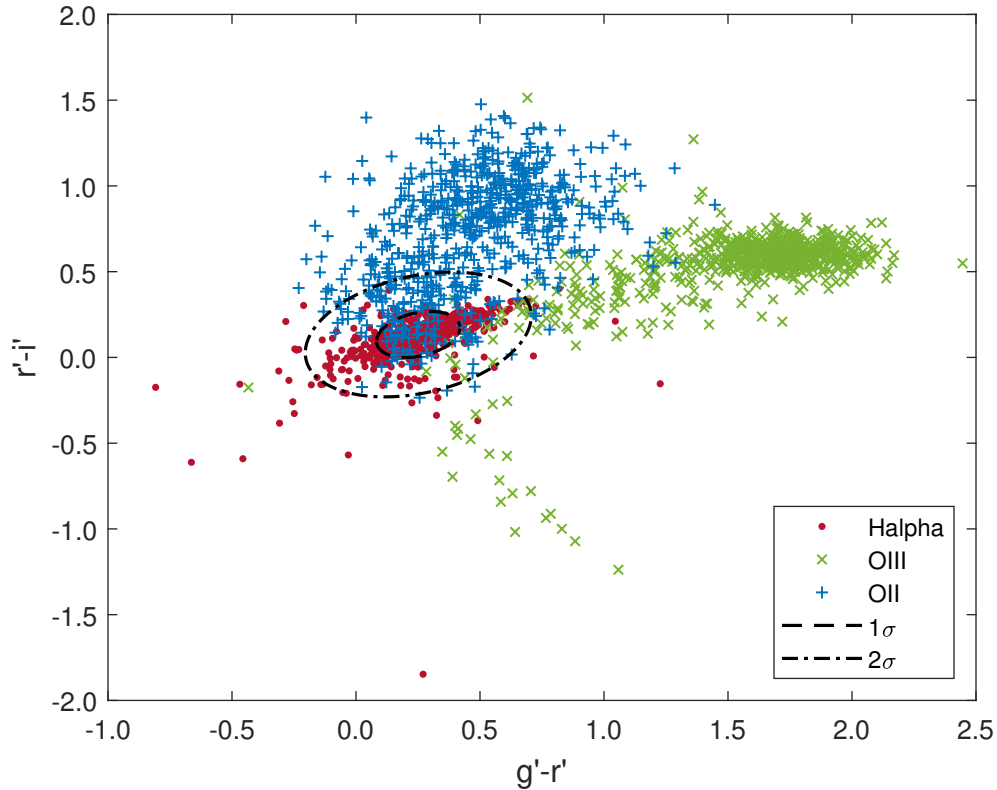


Figure 2.5 The color indices $g'-r'$ and $r'-i'$ of three populations of galaxies ($H\alpha$, [OIII] and [OII] emitting galaxies) plotted against each other. Each data point is a galaxy. The red group of galaxies are at a distance where the $H\alpha$ line is within the bandpass of the narrow Gaussian filters. The green dots are galaxies far enough away that the [OIII] line has been redshifted into the bandpass of the filters. The blue points are galaxies with the [OII] line redshifted into the bandpass of the filters. The above groups form three distinct (albeit overlapping) populations. The inner dashed circle shows the 1σ confidence region for $H\alpha$ galaxies and the outer dash dot circle shows the 2σ confidence region for the $H\alpha$ galaxies. The figure is from Draper et al. (2019)

many galaxies. Each point on the graph represents a galaxy with a known distance from SDSS. The x-axis is the $g'-r'$ color index of the galaxies, while the y-axis is their $r'-i'$ color index. The red dots represent galaxies at the correct redshift, or distance, for the $H\alpha$ emission line to be within the bandpass of our Narrow Gaussian filters. The green points are the galaxies at the distance where [OIII] is within the narrow filters' bandpasses. The blue dots are the galaxies that are even farther away so that the [OII] emission line is redshifted into the bandpass of our filters. The black dashed circle indicates the 1σ confidence region for the $H\alpha$ galaxies. The larger dash dot circle shows the 2σ confidence region for the $H\alpha$ galaxies. Of the galaxies within the 1σ region, 91.9% are $H\alpha$, 0.2% are [OIII] and 7.9% are [OII]. Within the 2σ region, 78.4% of the galaxies are $H\alpha$, 2.4% are [OIII] and are 19.2% [OII].

The galaxies in Figure 2.5 form three distinct (albeit slightly overlapping) populations, based on which emission line is being observed. Based on its color indices, each void galaxy candidate can be placed on this plot and sorted into one of the three groups ($H\alpha$, [OIII] or [OII]) with minimal uncertainty. Candidates that are determined to be $H\alpha$ emitters are kept as possible candidates. Objects that are [OIII] or [OII] emitters are discarded as false positives.

Chapter 3

Results and Discussion

3.1 Results

Using the narrowband filter method described in Section 2.1, we identified 2000 objects as potential void galaxy candidates. This means that our for each of these galaxies, if the emission line detected was in fact the $H\alpha$ line, then the galaxy is within the void. However, if it was another emission line detected, then the galaxy is far behind the void.

The broadband methods, described in Section 2.4, were used to determine which line was detected, and therefore, which candidates were actually in the void FN8. This is still an ongoing process. The most recent calculations have shown that 14 galaxies may be within the void. When these 14 objects were plotted on Figure 2.5 using their color indices, they all ended up in the region to the left of the 2σ region. This area, while sparsely populated, is almost solely populated by $H\alpha$ galaxies, so the 14 candidates found within that region have a low chance of being false positives. The candidates, however, do still need to be confirmed using spectroscopic observations.

3.2 Analysis

The Λ CDM model predicts that, while cosmological voids lack full-sized galaxies, the density of dwarf galaxies within the void should be the same as the density of regular galaxies outside the void, called a uniform distribution. With this assumption, we determined what percentage of the original 2000 candidates within FN8 should have been void galaxies, with the $H\alpha$ line being observed by the narrow filters, and how many should be false positives, with the [OIII] or [OII] lines within the bandpass of the narrow filters.

Figure 3.1 shows how significant the contribution from the [OIII] and [OII] galaxies behind the void is. Telescopes observe a certain field of view, which is an angular size. Imagine that the smallest square, closest to the Earth is the area of the void we see through a telescope. The telescope, however, can also see galaxies behind the void. The middle square, where the [OIII] emitters are, has a much greater survey area so, even though the galaxies are fainter because they are farther away, we still see more of them. The [OII] emitters are even farther away, so the area surveyed is even larger. meaning that even more galaxies can be observed and counted as false positives. Because we are looking at a larger patch of sky the farther we get from Earth, there are a lot of false positives within our 2000 candidates. It was my responsibility to calculate exactly how many there should be.

When calculating the expected number of void galaxies, I assumed, as the Λ CDM model predicts, that there was a uniform distribution of dwarf galaxies within the void FN8. I wrote a MATLAB program to find the expected number of galaxies in the void. This code is printed in Appendix B. There were many parameters that needed to be calculated to find the expected number of dwarf galaxies. The first was the density of galaxies there were in each of the three areas (see Figure 3.1) given a certain brightness. Brighter galaxies are less common and fainter galaxies are more common. To calculate this, I used an equation called the Schechter Function which requires certain constants. The constants I used came from the work of Hoyle et al. (2005).

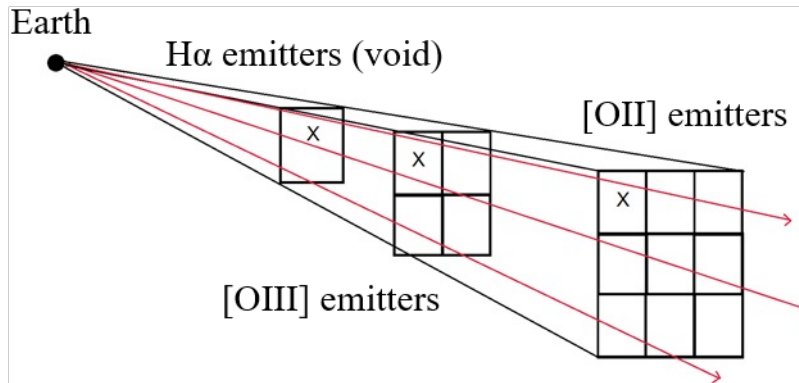


Figure 3.1 When we point a telescope towards the sky, the field of view is determined by a certain angle. The farther away the observer is looking, the more space can be encompassed by that field of view. [OIII] and [OII] galaxies that can be false positives in this method are behind the void. Because of this, many more [OIII] and [OII] emitting galaxies are within the field of view of the telescope than H α emitting galaxies, within the void. Adapted from: Sperrin & Winder (2014).

I then calculated how bright each galaxy would look from Earth to determine if it was bright enough for us to actually observe it. The volume of each region (for H α , [OIII] and [OII] emitters) was calculated to determine the number of galaxies within each region that were visible from Earth. With the number of H α , [OIII] and [OII] galaxies visible from Earth, I took the sum and found what percentage of the total were H α , [OIII] or [OII] galaxies.

I found that, assuming a uniform distribution of dwarf galaxies in the void, 46% of the candidates should have been [OIII] emitters (behind the void), 51% [OII] emitters (behind the void) and 2-3% H α emitters (within the void). It follows that, of the 2000 original candidates, 60 should have remained after the broadband test. Instead, we only found 14 candidate void galaxies. The 14 candidates we found represent 0.007% of the original 2000 candidates and 23% of the 60 dwarf galaxies expected. Even if all of the 14 candidates are confirmed to be within the void, the density of galaxies within the void is then only 23% of the cosmic mean rather than a uniform distribution (100% of the cosmic mean) predicted by Λ CDM.

3.3 Conclusions

Until now, no dwarf galaxies had been found inside intergalactic voids. The absence of void galaxies goes against the predictions of the Λ CDM model. It is difficult to observe these dwarf galaxies because they are so faint. We have developed a photometric method to survey for dwarf galaxies within intergalactic voids. Using this method, we have found 14 void galaxy candidates. This potential discovery of 14 void galaxies is unprecedented, but still requires further confirmation. Spectroscopic observations will be taken of these candidates as soon as possible to verify if they are within the void or simply false positives.

Even if these candidates are confirmed, our results show that the current cosmological model, Λ CDM, as well as our understanding of dark matter and how it influences galaxy formation must be refined. Some theories that addressed the apparent absence of dwarf galaxies were discussed in Section 1.3. Many of these are still viable to explain the scarcity of void galaxies that we now observe. Simpson et al. (2013) showed that supernovae explosions and UV background radiation from hot stars in the filaments could push gas out of the voids, quenching star and galaxy formation. Another theory is that dark matter, while predicted to be cold, is warmer than expected. Few dwarf galaxies can form in a universe where WDM dominates. Tinker & Conroy (2009) suggested that a simple galaxy bias, the requirement that dark matter halos must reach a certain mass before attracting baryonic matter, could solve the dwarf galaxy problem in voids. This would imply that there are dark matter halos in the voids, as predicted by Λ CDM, but not enough to form galaxies. Further work must be done to determine the exact cause of the scarcity of dwarf galaxies in voids.

3.4 Future Work

Because this method used is still being developed, the 14 galaxy candidates must be verified with spectroscopic observations. These observations will be done as soon as possible.

The observations done in this work were of the centers of voids. Another important question is how the density of galaxies falls off as you look into a void from a filament. How exactly does a dense intergalactic filament become an under-dense void? For my master's thesis at BYU, I will create the first-ever radial profile of a void. I will take observations of FN8 in a strip along the radius and, using the same methods from this work, will test these images to identify which galaxies are within or around the void. Finding this radial distribution of galaxies around the void will constrain which proposed theories explaining the absence of dwarf galaxies are actually possible.

Appendix A

Systematic Classification Code - VBA

A.1 CountKeep_Click()

```
Private Sub CountKeep_Click()
```

```
    Range("A:AK").Sort _  
        key1:=Range("Y:Y"), order1:=xlDescending, _  
        key2:=Range("AA:AA"), order2:=xlDescending, _  
        Header:=xlYes  
  
    For i = 2 To Rows.Count  
        If Worksheets("Objects").Cells(i, 27) = "no" _  
            And Worksheets("Objects").Cells(i, 25) = 0 Then  
            Range("A" & i & ":AK" & (Rows.Count)).Value = ""  
            Exit For  
        End If  
    End For
```

Next

End Sub

A.2 EW_Click()

Private Sub EW_Click()

 Range("A:AK").Sort _

 key1:=Range("Y:Y"), order1:=xlDescending, _

 key2:=Range("AI:AI"), order2:=xlDescending, _

 Header:=xlYes

For i = 2 To Rows.Count

If Worksheets("Objects").Cells(i, 35) = "delete" _

And Worksheets("Objects").Cells(i, 25) = 0 **Then**

 Range("A" & i & ":AK" & (Rows.Count)).Value = ""

Exit For

End If

Next

End Sub

A.3 FillInFormulas_Click()

Private Sub FillInFormulas_Click()

Dim lastRow As Long

lastRow = Range("A" & Rows.Count).End(xlUp).Row

'MagErr Keep

Range("Z2:Z" & lastRow).FormulaLocal = _

"=IF(MIN(E2,I2,M2)>=0.2,"no","yes")"

'Count Keep

Range("AA2:AA" & lastRow).FormulaLocal = _

"=IF(MAX(B2,F2,J2)<=500,"no","yes")"

'Ha8 Count Shifted

Range("AB2:AB" & lastRow).FormulaLocal = _

"=B2*Normalization!K\$2"

'Ha12 Count Shifted

Range("AC2:AC" & lastRow).FormulaLocal = _

"=F2*Normalization!N\$2"

'Ha16 Count Shifted

Range("AD2:AD" & lastRow).FormulaLocal = _

"=J2*Normalization!Q\$2"

'Ha12/Ha8

Range("AE2:AE" & lastRow).FormulaLocal = "=AC2/AB2"

'Ha12/Ha16

Range("AF2:AF" & lastRow).FormulaLocal = "=AC2/AD2"

'Physical Check

Range("AG2:AG" & lastRow).FormulaLocal = _

"=IF(AND(AE2<1,AF2<1),"delete","keep")"

'Min Value

Range("AH2:AH" & lastRow).FormulaLocal = _

"=IF(OR(AE2<0.01617,AF2<0.047001)," delete "," keep ")"

'EW

EWString = "=" _

& " IF (OR(IF (AND(AE2<=0.115755627009646,AF2<113.5),TRUE," _

& "FALSE)," _

& " IF (AND(AE2>0.115755627009646,AE2<=0.127239320165365," _

& "AF2<126),TRUE,FALSE)," _

& " IF (AND(AE2>0.127239320165365,AE2<=0.14850136239782," _

& "AF2<138.5),TRUE,FALSE)," _

& " IF (AND(AE2>0.14850136239782,AE2<=0.159854677565849," _

& "AF2<163.5),TRUE,FALSE)," _

& " IF (AND(AE2>0.159854677565849,AE2<=0.182561307901907," _

& "AF2<176),TRUE,FALSE)," _

& " IF (AND(AE2>0.182561307901907,AE2<=0.205267938237965," _

& "AF2<201),TRUE,FALSE)," _

& " IF (AND(AE2>0.205267938237965,AE2<=0.227974568574024," _

& "AF2<226),TRUE,FALSE)," _

& " IF (AND(AE2>0.227974568574024,AE2<=0.250681198910082," _

& "AF2<251),TRUE,FALSE)," _

& " IF (AND(AE2>0.250681198910082,AE2<=0.27338782924614," _

& "AF2<276),TRUE,FALSE)," _

& " IF (AND(AE2>0.27338782924614,AE2<=0.307447774750227," _

& "AF2<301),TRUE,FALSE),"

```
EWString = EWString _
    & " IF (AND(AE2>0.307447774750227 ,AE2<=0.330154405086285 , " _
        & " AF2<338.5) ,TRUE,FALSE) , " _
    & " IF (AND(AE2>0.330154405086285 ,AE2<=0.360125729681185 , " _
        & " AF2<26.9259259259259) ,TRUE,FALSE) , " _
    & " IF (AND(AE2>0.360125729681185 ,AE2<=0.39827429609446 , " _
        & " AF2<29.7037037037037) ,TRUE,FALSE) , " _
    & " IF (AND(AE2>0.39827429609446 ,AE2<=0.443687556766576 , " _
        & " AF2<32.4814814814815) ,TRUE,FALSE) , " _
    & " IF (AND(AE2>0.443687556766576 ,AE2<=0.472384373596767 , " _
        & " AF2<36.1851851851852) ,TRUE,FALSE) , " _
    & " IF (AND(AE2>0.472384373596767 ,AE2<=0.506061966771441 , " _
        & " AF2<38.962962962963) ,TRUE,FALSE) , " _
    & " IF (AND(AE2>0.506061966771441 ,AE2<=0.539739559946116 , " _
        & " AF2<41.7407407407407) ,TRUE,FALSE) , " _
    & " IF (AND(AE2>0.539739559946116 ,AE2<=0.579927338782925 , " _
        & " AF2<44.5185185185185) ,TRUE,FALSE) , " _
    & " IF (AND(AE2>0.579927338782925 ,AE2<=0.607094746295465 , " _
        & " AF2<47.2962962962963) ,TRUE,FALSE) , " _
    & " IF (AND(AE2>0.607094746295465 ,AE2<=0.640772339470139 , " _
        & " AF2<50.0740740740741) ,TRUE,FALSE) , " _
    & " IF (AND(AE2>0.640772339470139 ,AE2<=0.674449932644814 , " _
        & " AF2<27.4423076923077) ,TRUE,FALSE) , " _
    & " IF (AND(AE2>0.674449932644814 ,AE2<=0.708127525819488 , " _
        & " AF2<28.8846153846154) ,TRUE,FALSE) , "
```

```
EWString = EWString _
& " IF (AND(AE2>0.708127525819488 ,AE2<=0.738873751135331 , " _
& " AF2<30.3269230769231),TRUE,FALSE) , " _
& " IF (AND(AE2>0.738873751135331 ,AE2<=0.764256847777279 , " _
& " AF2<21.1298701298701),TRUE,FALSE) , " _
& " IF (AND(AE2>0.764256847777279 ,AE2<=0.806993642143506 , " _
& " AF2<22.1038961038961),TRUE,FALSE) , " _
& " IF (AND(AE2>0.806993642143506 ,AE2<=0.818346957311535 , " _
& " AF2<23.0779220779221),TRUE,FALSE) , " _
& " IF (AND(AE2>0.818346957311535 ,AE2<=0.841053587647593 , " _
& " AF2<17.6666666666667),TRUE,FALSE) , " _
& " IF (AND(AE2>0.841053587647593 ,AE2<=0.863760217983651 , " _
& " AF2<18.156862745098),TRUE,FALSE) , " _
& " IF (AND(AE2>0.863760217983651 ,AE2<=0.886466848319709 , " _
& " AF2<14.9763779527559),TRUE,FALSE) , " _
& " IF (AND(AE2>0.886466848319709 ,AE2<=0.897820163487738 , " _
& " AF2<15.3700787401575),TRUE,FALSE) , " _
& " IF (AND(AE2>0.897820163487738 ,AE2<=0.919614147909968 , " _
& " AF2<13.0065789473684),TRUE,FALSE) , " _
& " IF (AND(AE2>0.919614147909968 ,AE2<=0.931097841065687 , " _
& " AF2<11.3107344632768),TRUE,FALSE) , " _
& " IF (AND(AE2>0.931097841065687 ,AE2<=0.942581534221406 , " _
& " AF2<10.0346534653465),TRUE,FALSE) , " _
& " IF (AND(AE2>0.942581534221406 ,AE2<=0.954065227377125 , " _
& " AF2<8.14285714285714),TRUE,FALSE) , "
```



```
EWString = EWString _
    & " IF (AND(AE2>0.954065227377125 ,AE2<=0.976765799256506 , " _
        & " AF2<5.90056818181818),TRUE,FALSE) , " _
    & " IF (AND(AE2>0.976765799256506 ,AE2<=0.988246356370475 , " _
        & " AF2<4.65044247787611),TRUE,FALSE) , " _
    & " IF (AND(AE2>0.988246356370475 ,AE2<=1 , " _
        & " AF2<4.18725099601594),TRUE,FALSE) , " _
    & " IF (AND(AE2>1 ,AE2<=1.01189343482398 , " _
        & " AF2<3.80797101449275),TRUE,FALSE) , " _
    & " IF (AND(AE2>1.01189343482398 ,AE2<=1.02436647173489 , " _
        & " AF2<3.53322259136213),TRUE,FALSE) , " _
    & " IF (AND(AE2>1.02436647173489 ,AE2<=1.03700049333991 , " _
        & " AF2<3.2239263803681),TRUE,FALSE) , " _
    & " IF (AND(AE2>1.03700049333991 ,AE2<=1.06322711178553 , " _
        & " AF2<2.99430199430199),TRUE,FALSE) , " _
    & " IF (AND(AE2>1.06322711178553 ,AE2<=1.0640368852459 , " _
        & " AF2<2.70527670527671),TRUE,FALSE) , " _
    & " IF (AND(AE2>1.0640368852459 ,AE2<=1.09081473793461 , " _
        & " AF2<2.51148730350665),TRUE,FALSE) , " _
    & " IF (AND(AE2>1.09081473793461 ,AE2<=1.11987213638785 , " _
        & " AF2<2.33037694013304),TRUE,FALSE) , " _
    & " IF (AND(AE2>1.11987213638785 ,AE2<=1.16648168701443 , " _
        & " AF2<2.15148413510747),TRUE,FALSE) , " _
    & " IF (AND(AE2>1.16648168701443 ,AE2<=1.19977168949772 , " _
        & " AF2<1.99809885931559),TRUE,FALSE) , "
```

```
EWString = EWString _  
& " IF (AND(AE2>1.19977168949772 ,AE2<=1.25342874180083 ,"  
    & " AF2<1.86512866015972),TRUE,FALSE) , " _  
& " IF (AND(AE2>1.25342874180083 ,AE2<=1.30731407498463 ,"  
    & " AF2<1.74875207986689),TRUE,FALSE) , " _  
& " IF (AND(AE2>1.30731407498463 ,AE2<=1.35438144329897 ,"  
    & " AF2<1.66562255285826),TRUE,FALSE) , " _  
& " IF (AND(AE2>1.35438144329897 ,AE2<=1.44008124576845 ,"  
    & " AF2<1.55473372781065),TRUE,FALSE) , " _  
& " IF (AND(AE2>1.44008124576845 ,AE2<=1.51711840228245 ,"  
    & " AF2<1.49053959355291),TRUE,FALSE) , " _  
& " IF (AND(AE2>1.51711840228245 ,AE2<=1.58402411454408 ,"  
    & " AF2<1.41611185086551),TRUE,FALSE) , " _  
& " IF (AND(AE2>1.58402411454408 ,AE2<=1.69888178913738 ,"  
    & " AF2<1.33291058972733),TRUE,FALSE) , " _  
& " IF (AND(AE2>1.69888178913738 ,AE2<=1.84635416666667 ,"  
    & " AF2<1.30731407498463),TRUE,FALSE) , " _  
& " IF (AND(AE2>1.84635416666667 ,AE2<=1.97493036211699 ,"  
    & " AF2<1.2497062279671),TRUE,FALSE) , " _  
& " IF (AND(AE2>1.97493036211699 ,AE2<=2.12275449101796 ,"  
    & " AF2<1.1969611705121),TRUE,FALSE) , " _  
& " IF (AND(AE2>2.12275449101796 ,AE2<=2.29449838187702 ,"  
    & " AF2<1.16420361247947),TRUE,FALSE) , " _  
& " IF (AND(AE2>2.29449838187702 ,AE2<=2.45381984036488 ,"  
    & " AF2<1.11829652996845),TRUE,FALSE) , "
```

```
EWString = EWString _
    & " IF (AND(AE2>2.45381984036488 ,AE2<=2.68329177057357 , " _
        & " AF2<1.10245901639344) ,TRUE,FALSE) , " _
    & " IF (AND(AE2>2.68329177057357 ,AE2<=2.92572214580468 , " _
        & " AF2<1.06166748889985) ,TRUE,FALSE) , " _
    & " IF (AND(AE2>2.92572214580468 ,AE2<=3.26226993865031 , " _
        & " AF2<1.04933399111988) ,TRUE,FALSE) , " _
    & " IF (AND(AE2>3.26226993865031 ,AE2<=3.57475083056478 , " _
        & " AF2<1.02407318247472) ,TRUE,FALSE) , " _
    & " IF (AND(AE2>3.57475083056478 ,AE2<=4.45911949685535 , " _
        & " AF2<1.02378686964795) ,TRUE,FALSE) , " _
    & " IF (AND(AE2>4.45911949685535 ,AE2<=4.76106194690265 , " _
        & " AF2<0.988382899628253) ,TRUE,FALSE) , " _
    & " IF (AND(AE2>4.76106194690265 ,AE2<=5.35323383084577 , " _
        & " AF2<0.988516306844281) ,TRUE,FALSE) , " _
    & " IF (AND(AE2>5.35323383084577 ,AE2<=6.18465909090909 , " _
        & " AF2<0.977293369663942) ,TRUE,FALSE) , " _
    & " IF (AND(AE2>6.18465909090909 ,AE2<=6.58103975535168 , " _
        & " AF2<0.977548271216884) ,TRUE,FALSE) , " _
    & " IF (AND(AE2>6.58103975535168 ,AE2<=9.48017621145375 , " _
        & " AF2<0.977293369663942) ,TRUE,FALSE) , " _
    & " IF (AND(AE2>9.48017621145375 ,AE2<=12.0169491525424 , " _
        & " AF2<0.966322406825326) ,TRUE,FALSE) , " _
    & " IF (AND(AE2>12.0169491525424 ,AE2<=13.8289473684211 , " _
        & " AF2<0.955096542433767) ,TRUE,FALSE) , "
```

```

EWString = EWString _
    & " IF (AND(AE2>13.8289473684211,AF2<0.943870678042209)," _
        & "TRUE,FALSE))," "keep"," "delete"")"
Range("AI2:AI" & lastRow).FormulaLocal = EWString
'In Circle?
Range("AJ2:AJ" & lastRow).FormulaLocal = _
    "=IF(AF2<($AN$31*(AE2-$AN$29)/$AN$28+" _
    & "SQRT(((AE2-$AN$29)/$AN$28)^2*($AN$31^2-1)-" _
    & "(1/$AR$29)*LN($AR$30/$AR$28)))*" _
    & "$AO$28+$AO$29," "delete"," "keep"")"
'Select
Range("AK2:AK" & lastRow).FormulaLocal = _
    "=IF(AND(P2>AW$6,P2<AX$6,Q2>AY$6,Q2<AZ$6,T2<4),1,0)"

```

End Sub

A.4 FindConstant_Click()

```
Private Sub FindConstant_Click()
```

```

    oldDifference = 100
    Dim constant As Variant

    For i = 1 To 9
        Range("AR30").Value = "." & i
        Percent = Range("AR35").Value

```

```
difference = Abs(0.95 - Percent)
If difference > oldDifference Then
    Range("AR30").Value = "." & i - 1
    constant = 0.1 * (i - 1)
    Exit For
Else
    oldDifference = difference
End If
Next

oldDifference = 100
For i = -9 To 9
    Range("AR30").Value = constant + (0.01 * i)
    Percent = Range("AR35").Value
    difference = Abs(0.95 - Percent)
    If difference > oldDifference Then
        Range("AR30").Value = constant + (0.01 * i) - 0.01
        constant = constant + (0.01 * i) - 0.01
        Exit For
    Else
        oldDifference = difference
    End If
Next

oldDifference = 100
```

```
For i = -9 To 9
    Range("AR30").Value = constant + (0.001 * i)
    Percent = Range("AR35").Value
    difference = Abs(0.95 - Percent)
    If difference > oldDifference Then
        Range("AR30").Value = constant + (0.001 * i) - 0.001
        constant = constant + (0.001 * i) - 0.001
        Exit For
    Else
        oldDifference = difference
    End If
Next

End Sub
```

A.5 FindCorrelation_Click()

```
Private Sub FindCorrelation_Click ()

    Dim corr As Long
    lastRow = (Cells.CurrentRegion.Rows.Count)
    firstRow = 0
    i = 1

    Do While firstRow = 0
        If Worksheets("Objects").Cells(i, 25) = 0 Then
```

```

        firstRow = i
    Else
        i = i + 1
    End If
Loop

Application.Run "ATPVBAEN.XLAM! Mcorrel", _
    Range("AE" & firstRow & ":AF" & lastRow), _
    Range("AW9"), "C", False

```

End Sub

A.6 MagErrKeep_Click()

Private Sub MagErrKeep_Click()

```

Range("A:AK").Sort _
    key1:=Range("Y:Y"), order1:=xlDescending, _
    key2:=Range("Z:Z"), order2:=xlDescending, _
    Header:=xlYes

For i = 2 To Rows.Count
    If Worksheets("Objects").Cells(i, 26) = "no" And _
        Worksheets("Objects").Cells(i, 25) = 0 Then
        Range("A" & i & ":AK" & (Rows.Count)).Value = ""
    
```

```
        Exit For
    End If
Next
End Sub
```

A.7 MinValue_Click()

```
Private Sub MinValue_Click()

    Range("A:AK").Sort _
        key1:=Range("Y:Y"), order1:=xlDescending, _
        key2:=Range("AH:AH"), order2:=xlDescending, _
        Header:=xlYes

    For i = 2 To Rows.Count
        If Worksheets("Objects").Cells(i, 34) = "delete" And _
            Worksheets("Objects").Cells(i, 25) = 0 Then
            Range("A" & i & ":AK" & (Rows.Count)).Value = ""
            Exit For
        End If
    Next

End Sub
```

A.8 PhysicalCheck_Click()


```
Private Sub PhysicalCheck_Click()
```

```
    Range("A:AK").Sort _  
        key1:=Range("Y:Y"), order1:=xlDescending, _  
        key2:=Range("AG:AG"), order2:=xlDescending, _  
        Header:=xlYes  
  
    For i = 2 To Rows.Count  
        If Worksheets("Objects").Cells(i, 33) = "delete" And _  
            Worksheets("Objects").Cells(i, 25) = 0 Then  
            Range("A" & i & ":AK" & (Rows.Count)).Value = ""  
            Exit For  
        End If  
    Next
```

```
End Sub
```

A.9 SelectColumn_Click()

```
Private Sub SelectColumn_Click()
```

```
    Range("A:AK").Sort _  
        key1:=Range("Y:Y"), order1:=xlDescending, _  
        key2:=Range("AK:AK"), order2:=xlDescending, _  
        Header:=xlYes
```

```
For i = 2 To Rows.Count
    If Worksheets("Objects").Cells(i, 37) = 0 And _
        Worksheets("Objects").Cells(i, 25) = 0 Then
        Range("A" & i & ":AK" & (Rows.Count)).Value = ""
    Exit For
End If
Next
```

```
End Sub
```

A.10 StDevAndMedian_Click()

```
Private Sub StDevAndMedian_Click()
```

```
    lastRow = (Rows.Count)
    firstRow = 0
    i = 1

    Do While firstRow = 0
        If Worksheets("Objects").Cells(i, 25) = 0 Then
            firstRow = i
        Else
            i = i + 1
        End If
    Loop
```

```
Range("AN28:AN28").FormulaLocal = _
    "=STDEV(AE" & firstRow & ":AE" & lastRow & ")"
Range("AO28:AO28").FormulaLocal = _
    "=STDEV(AF" & firstRow & ":AF" & lastRow & ")"
Range("AN29:AN29").FormulaLocal = _
    "=MEDIAN(AE" & firstRow & ":AE" & lastRow & ")"
Range("AO29:AO29").FormulaLocal = _
    "=MEDIAN(AF" & firstRow & ":AF" & lastRow & ")"
Range("AR28:AR28").FormulaLocal = _
    "=1/(2*PI()*AN28*AO28*SQRT(1-AN31^2))"
Range("AR29:AR29").FormulaLocal = _
    "=1/(2*(1-AN31^2))"
Range("AR33:AR33").FormulaLocal = _
    "=COUNTIF(AJ$" & firstRow & ":AE$" _
    & lastRow & ", "delete")"
```

End Sub

Appendix B

Expected Numbers Code - MATLAB

B.1 ExpectedNumberofGalaxiesTOTAL.m

```
%%%%%%%%%%%%%%%%%%%%%%%%%%%%%%%%%%%%%%%%%%%%%%%%%%%%%%%%%%%%%%%%%%%%%%%%%  
%%  
%% EXPECTED NUMBER OF GALAXIES TOTAL %%  
%%%%%%%%%%%%%%%%%%%%%%%%%%%%%%%%%%%%%%%%%%%%%%%%%%%%%%%%%%%%%%%%%%%%%%%%
```

```
% This script calculates what percentage of galaxies we detect  
% are Halpha emission , OIII emission and OII emission . This  
% script uses the files :  
% ExpectedNumberofGalaxiesHa .m  
% ExpectedNumberofGalaxiesOIII .m  
% ExpectedNumberofGalaxiesOII .m  
% Schechter .m
```

```
clear ; close all ;
```



```
%% OTHER PARAMETERS %%
```

```
%%%%%%%%%%%%%%%%%%%%%%%%%%%%%%%%%%%%%%%%%%%%%%%%%%%%%%%%%%%%%%%%%%%%%%%%
```

```
bin = 0.1;
```

```
M = -22:bin:-9.4;
```

```
phistar = phistar*bin;
```

```
N = length(M);
```

```
% Necessary Parameters:
```

```
% c, FOV, sphere, H0, q0, Mstar, alpha, phistar, SurveyDepth, EW,
```

```
% M, N
```

```
% Run the files for Ha, OII and OIII
```

```
[HaNum,NHa] = ...
```

```
    ExpectedNumberofGalaxiesHa(c, FOV, sphere, H0, q0, Mstar, ...  
    alpha, phistar, SurveyDepth, EW, M);
```

```
[OIIINum,NOIII] =...
```

```
    ExpectedNumberofGalaxiesOIII(c, FOV, sphere, H0, q0, ...  
    Mstar, alpha, phistar, SurveyDepth, EW, M);
```

```
[OIINum,NOII] =...
```

```
    ExpectedNumberofGalaxiesOII(c, FOV, sphere, H0, q0, Mstar, ...  
    alpha, phistar, SurveyDepth, EW, M);
```

```
HaPercent = 100*HaNum/(HaNum+OIIINum+OIINum);
```

```
OIIIPercent = 100*OIIINum/(HaNum+OIIINum+OIINum);
```



```
%%%%%%%%%%%%%%%%%%%%%%%%%%%%%%%%%%%%%%%%%%%%%%%%%%%%%%%%%%%%%%%%%%%%%%%%%
```

```
%%% OTHER PARAMETERS %%%
```

```
%%%%%%%%%%%%%%%%%%%%%%%%%%%%%%%%%%%%%%%%%%%%%%%%%%%%%%%%%%%%%%%%%%%%%%%%%
```

```
czHalpHa = 700:100:9400; % km/s, redshift
```

```
% Get the LMF from Schechter function
```

```
LMF = Schechter(Mstar, phistar, alpha, M); % # of galaxies per Mpc^2
```

```
%%%%%%%%%%%%%%%%%%%%%%%%%%%%%%%%%%%%%%%%%%%%%%%%%%%%%%%%%%%%%%%%%%%%%%%%%
```

```
%% Find the volume of each section %%
```

```
%%%%%%%%%%%%%%%%%%%%%%%%%%%%%%%%%%%%%%%%%%%%%%%%%%%%%%%%%%%%%%%%%%%%%%%%%
```

```
% Find proper distance (Mpc)
```

```
dp = (czHalpHa - (1/2)*(1+q0)*(czHalpHa).^2/c)/H0;
```

```
% Mpc, proper distance
```

```
% Find volume of cones (Mpc^3)
```

```
vol = (4/3)*pi*dp.^3*(FOV/sphere); % Mpc, volumes of cones
```

```
% Find luminosity distance (km/s)
```

```
dL = czHalpHa + (1/2)*(1-q0)*czHalpHa.^2/c;
```

```
%km/s, luminosity distance
```

```
% Find volumes between the cones
```



```
deltaVol=zeros(1,length(vol)-1);
for i=1:length(vol)-1
    deltaVol(i)=vol(i+1)-vol(i);
end

% Next, I need to figure out how what fraction of the galaxies
% have a certain EW of H alpha emission.

HalpowerLaw = @(x) 27.93*x^(-2.00);
% From "Expected numbers of galaxies.xlsx"
EmissionPowerLaw = HalpowerLaw(EW);
FracwEmission = EmissionPowerLaw;

% Calculate the total number of galaxies

% The number of galaxies with emission is presented in a matrix
% Each column has a different absolute magnitude
% Each row has a different distance
for i=1:length(deltaVol)
    NumwEmission(i,:) = LMF.*FracwEmission.*deltaVol(i);
end

% Also find the apparent magnitudes of the galaxies at certain
% distances, given their absolute magnitudes.
```

```

appMag = ...
    @(cznear , czfar) M+5*log10((cznear+czfar)/2) - 5*log10(H0)+25;

for i=1:length(deltaVol)
    m(i,:) = appMag(dL(i),dL(i+1));
end

MCopy = zeros(length(deltaVol),length(M));
for i=1:length(deltaVol)
    MCopy(i,:)=M;
end

% Pick the indices that m<23, and add those up in the
% NumwEmission matrix
for i=1:length(deltaVol)
    for j=1:length(M)
        if m(i,j)>SurveyDepth
            NumwEmission(i,j)=0;
            MCopy(i,j) = 0;
        end
    end
end

end

% Add up all the different pieces of
theSum=sum(NumwEmission); % vector

```

```
theSum=sum(theSum); % number
```

```
F=theSum;
```

B.3 ExpectedNumberofGalaxiesOIII.m

```
%%%%%%%%%%%%%%%%%%%%%%%%%%%%%%%%%%%%%%%%%%%%%%%%%%%%%%%%%%%%%%%%%%%%%%%%%%
```

```
%%% EXPECTED NUMBER OF GALAXIES OIII %%%
```

```
%%%%%%%%%%%%%%%%%%%%%%%%%%%%%%%%%%%%%%%%%%%%%%%%%%%%%%%%%%%%%%%%%%%%%%%%%%
```

```
function [F, NumwEmission]=...
```

```
    ExpectedNumberofGalaxiesOIII(c, FOV, sphere, H0, q0, ...
```

```
    Mstar, alpha, phistar, SurveyDepth, EW, M)
```

```
% This is a script to determine the number of galaxies that we
```

```
% find in the filters we would expect would be OIII emission.
```

```
clear LMF dp vol dL deltaVol FracwEmission NumwEmission appMag...
```

```
    m theSum PercentByMag
```

```
format long
```

```
%%%%%%%%%%%%%%%%%%%%%%%%%%%%%%%%%%%%%%%%%%%%%%%%%%%%%%%%%%%%%%%%%%%%%%%%%%
```

```
%%% OTHER PARAMETERS %%%
```

```
%%%%%%%%%%%%%%%%%%%%%%%%%%%%%%%%%%%%%%%%%%%%%%%%%%%%%%%%%%%%%%%%%%%%%%%%%%
```

```
czOIII=94100:100:105600; % km/s, redshift
```

```
% Get the LMF from Schechter function
```

LMF = Schechter(Mstar , phistar , alpha ,M); % # of galaxies per Mpc²

% Find the volume of each section

% Find proper distance (Mpc)

% Find volume of cones (Mpc³)

% Find luminosity distance (km/s)

% Find volumes between the cones

% Next, I need to figure out how what fraction of the galaxies

% have a certain EW of H OIII emission.

% Find the volume of each section

% Find proper distance (Mpc)

% Find volume of cones (Mpc³)

% Find luminosity distance (km/s)

% Find volumes between the cones

% Next, I need to figure out how what fraction of the galaxies

% have a certain EW of H OIII emission.

end

% Next, I need to figure out how what fraction of the galaxies

% have a certain EW of H OIII emission.

```
OIIIPowerLaw = @(x) 2.88*x^(-1.52);
% From "Expected numbers of galaxies.xlsx"
EmissionPowerLaw = OIIIPowerLaw(EW);
FracwEmission = EmissionPowerLaw;

% Calculate the total number of galaxies

% The number of galaxies with emission is presented in a matrix
% Each column has a different absolute magnitude
% Each row has a different distance
for i=1:length(deltaVol)
    NumwEmission(i,:) = LMF.*FracwEmission.*deltaVol(i);
end

% Also find the apparent magnitudes of the galaxies at certain
% distances, given their absolute magnitudes.

appMag = ...
    @(cznear, czfar) M+5*log10((cznear+czfar)/2)-5*log10(H0)+25;

for i=1:length(deltaVol)
    m(i,:) = appMag(dL(i), dL(i+1));
end

MCopy = zeros(length(deltaVol), length(M));
```

```

for i=1:length(deltaVol)
    MCopy(i,:)=M;
end

% Pick the indices that m<23, and add those up in the
% NumwEmission matrix
for i=1:length(deltaVol)
    for j=1:length(M)
        if m(i,j)>SurveyDepth
            NumwEmission(i,j)=0;
            MCopy(i,j)=0;
        end
    end
end

% Add up all the different pieces of
theSum=sum(NumwEmission);
theSum=sum(theSum);
F = theSum;

```

B.4 ExpectedNumberofGalaxiesOII.m

```

%/%/% EXPECTED NUMBER OF GALAXIES OII %/%/%

```

```

function [F, NumwEmission ] = ...
    ExpectedNumberofGalaxiesOII(c, FOV, sphere , H0, q0, Mstar , ...
    alpha , phistar , SurveyDepth , EW, M)

% This is a script to determine the number of galaxies that we
% find in the filters we would expect would be OII emission.

clear LMF dp vol dL deltaVol FracwEmission NumwEmission ...
    appMag m theSum PercentByMag

format long

%%%%%%%%%%%%%%%%%%%%%%%%%%%%%%%%%%%%%%%%%%%%%%%%%%%%%%%%%%%%%%%%%%%%%%%%%
%%% OTHER PARAMETERS %%%
%%%%%%%%%%%%%%%%%%%%%%%%%%%%%%%%%%%%%%%%%%%%%%%%%%%%%%%%%%%%%%%%%%%%%%%%%
    czOII=229500:100:244900; % km/s, redshift

% Get the LMF from Schechter function
    LMF = Schechter(Mstar , phistar , alpha ,M); % # of galaxies per Mpc^2

%%%%%%%%%%%%%%%%%%%%%%%%%%%%%%%%%%%%%%%%%%%%%%%%%%%%%%%%%%%%%%%%%%%%%%%%%
%%% Find the volume of each section %%%
%%%%%%%%%%%%%%%%%%%%%%%%%%%%%%%%%%%%%%%%%%%%%%%%%%%%%%%%%%%%%%%%%%%%%%%%%

% Find proper distance (Mpc)
    dp = (czOII - (1/2)*(1+q0)*(czOII).^2/c)/H0; % Mpc, proper distance

```

```

% Find volume of cones (Mpc^3)
vol = (4/3)*pi*dp.^3*(FOV/sphere); % Mpc, volumes of cones

% Find luminosity distance (km/s)
dL = czOII+(1/2)*(1-q0)*czOII.^2/c; %km/s, luminosity distance

% Find volumes between the cones
deltaVol=zeros(1,length(vol)-1);
for i=1:length(vol)-1
    deltaVol(i)=vol(i+1)-vol(i);
end

% Next, I need to figure out how what fraction of the galaxies
% have a certain EW of OII emission.

OIIPowerLaw = @(x) 22.65*x^(-1.75);
% From "Expected numbers of galaxies.xlsx"
EmissionPowerLaw = OIIPowerLaw(EW);
FracwEmission = EmissionPowerLaw;

% Calculate the total number of galaxies

% The number of galaxies with emission is presented in a matrix
% Each column has a different absolute magnitude

```



```
% Each row has a different distance
for i=1:length(deltaVol)
    NumwEmission(i,:) = LMF.*FracwEmission.*deltaVol(i);
end

% Also find the apparent magnitudes of the galaxies at certain
% distances, given their absolute magnitudes.

appMag = ...
    @(cznear, czfar) M+5*log10((cznear+czfar)/2) - 5*log10(H0)+25;

for i=1:length(deltaVol)
    m(i,:) = appMag(dL(i), dL(i+1));
end

MCopy = zeros(length(deltaVol), length(M));
for i=1:length(deltaVol)
    MCopy(i,:)=M;
end

% Pick the indices that m<23, and add those up in the
% NumwEmission matrix
for i=1:length(deltaVol)
    for j=1:length(M)
        if m(i,j)>SurveyDepth
```

```

        NumwEmission(i , j)=0;
        MCopy(i , j)=0;
    end
end
end

% Add up all the different pieces of
theSum=sum(NumwEmission);
theSum=sum(theSum);
F = theSum;

```

B.5 Schechter.m

```

function F=Schechter(Mstar , phistar , alpha ,M)

%%% This is the Schechter function

F=(2/5)* phistar .* log(10).*(10.^((2/5).*(Mstar-M)))...
    .^(alpha+1).* exp(-10.^((2/5).*(Mstar-M)));

```

Bibliography

Abolfathi, B., et al. 2018, ApJS, 235, 42

Bertin, E., & Arnouts, S. 1996, Astron. Astrophys. Suppl. Ser., 117, 393

Carroll, B. W., & Ostlie, D. A. 2007, An Introduction to Modern Astrophysics, 2nd edn., ed. A. R. S. Black (Glenview, IL: Pearson Education Inc.)

Draper, C. D., et al. 2019, (in prep)

Foster, C., & Nelson, L. A. 2009, Astrophys. J., 699, 1252

Hinshaw, G., et al. 2013, ApJS, 208

Hoyle, F., et al. 2005, Astrophys. J., 620, 618

J. S. Bullock, M. B.-K. 2017, Annu. Rev. Astron. Astrophys., 55, 343

Maran, S. P., ed. 1992, The Astronomy and Astrophysics Encyclopedia (Oakleigh, Australia: Cambridge University Press)

Schaye, J., et al. 2015, MNRAS, 446, 521

Simpson, C. M., et al. 2013, MNRAS, 432, 1989

Sperrin, M., & Winder, J. 2014, Scientific Basis of the Royal College of Radiologists Fellowship: Illustrated questions and answers (Bristol,UK: Institute of Physics Publishing)

Tikhonov, A. V., & Klypin, A. 2009, MNRAS, 395, 1915

Tinker, J. L., & Conroy, C. 2009, *Astrophys. J.*, 691, 633

Vogelsberger, M., et al. 2014, MNRAS, 444, 1518

Index

Λ CDM model, 1, 3, 25–27
[OIII], 4, 5, 21–23, 25, 26
[OII], 4, 5, 21–23, 25, 26
Broadband Filters, 21, 24
Cosmological Redshift, 6, 7, 13, 17, 21
Dark Matter, 1–3, 9, 27
 cold, 2, 3
 hot, 2, 3
 warm, 2, 3
Dwarf Galaxy, 16, 25, 27
Equivalent Width, 5, 13, 17, 18, 20, 21
 $H\alpha$, 4, 5, 11–13, 21–26
 ratios, 11–14, 16–18
Narrow Gaussian Filters, 11, 13, 14, 21, 24
Photometry, 7, 8, 13, 21, 27
Spectroscopy, 4, 7, 21, 24, 27
Systematic Classification, 13, 16
Visual Survey, 13, 14
Voids, 25, 27, 28
 definition, 4
 FN2, 11
 FN8, 11, 24, 28
 void galaxy, 10, 13–16, 23–25, 27